Inhibition of IRAK1 Ubiquitination Determines Glucocorticoid Sensitivity for TLR9-Induced Inflammation in Macrophages

Fansheng Kong,* Zhiwei Liu,[†] Viral G. Jain,[‡] Kenjiro Shima,[§] Takuji Suzuki,[§] Louis J. Muglia,* Daniel T. Starczynowski,[¶] Chandrashekhar Pasare,[‖] and Sandip Bhattacharyya*

Inflammatory responses are controlled by signaling mediators that are regulated by various posttranslational modifications. Recently, transcription-independent functions for glucocorticoids (GC) in restraining inflammation have emerged, but the underlying mechanisms are unknown. In this study, we report that GC receptor (GR)–mediated actions of GC acutely suppress TLR9-induced inflammation via inhibition of IL-1R–associated kinase 1 (IRAK1) ubiquitination. β-TrCP–IRAK1 interaction is required for K48-linked ubiquitination of IRAK1 at Lys^{134} and subsequent membrane-to-cytoplasm trafficking of IRAK1 interacting partners TNFR-associated factor 6 and TAK1 that facilitates NF-κB and MAPK activation. Upon costimulation of macrophages with GC and TLR9-engaging ligand, GR physically interacts with IRAK1 and interferes with protein–protein interactions between β-TrCP and IRAK1. Ablation of GR in macrophages prevents GC-dependent suppression of β-TrCP–IRAK1 interactions. This GC-mediated suppression of IRAK1 activation is unique to TLR9, as GC treatment impairs TLR9 but not TLR4 ligand–induced K48-linked IRAK1 ubiquitination and trafficking of IRAK1 interacting partners. Furthermore, mutations in IRAK1 at Lys^{134} prevent TLR9 ligand–induced activation of inflammatory signaling mediators and synthesis of proinflammatory cytokines to an extent comparable to GC-mediated inhibition. Collectively, these findings identify a transcription-independent, rapid, and nongenomic GC suppression of TLR9 ligand–mediated IRAK1 ubiquitination as a novel mechanism for restraining acute inflammatory reactions. *The Journal of Immunology*, 2017, 199: 3654–3667.

Glucocorticoids (GC), produced endogenously or administered therapeutically, provide a necessary restraint to inflammatory disorders (1, 2). Although transcription-dependent genomic functions of GC have been thoroughly characterized, rapid, nongenomic actions of GC in restraining inflammation are emerging (3–5). In acute stress, mounting evidence suggests that nongenomic GC activities provide therapeutic benefits (6). The beneficial nongenomic GC effects have been implicated in asthma, allergic rhinitis, cardiovascular pathologies, and rheumatoid arthritis (7–10). In fact, GC suppress aerosol-mediated allergic asthma within 10 min of challenge with allergen (11), and macrophage potency for phagocytosis and reactive oxygen species generation were inhibited within 30 min of GC treatment (12). Also, GC inhibited fMLF-induced neutrophil degranulation within 5 min of ligand treatment (13). However, the mechanisms involved in nongenomic GC functions that control acute inflammatory stresses remain elusive.

TLRs are molecular sensors that recognize both intracellular and extracellular stress signals. Unrestrained activation of TLRs occurs in numerous inflammatory disorders (14, 15). A wealth of studies implicated GC interference with TLR ligand–mediated immune actions (16), including targeting of GRIP1–IFN regulatory factor 3 interactions (17), microRNA (18), dendritic cell maturation (19), and systemic lupus erythematosus (20). We have demonstrated that both in vivo and in vitro, in comparison with TLR ligands, such as CpG (TLR9 ligand) or polyinosinic-polycytidylic acid [poly(I:C); TLR3 ligand], treatment with GC contributes to limited potency in restricting LPS (TLR4 ligand)–mediated inflammatory reactions (21). Furthermore, we found that GC inhibition of ligand-induced activation of inflammatory signaling mediators, such as TAK1, NF-κB, and MAPK, occurred within minutes after TLR engagement (21–23). These data suggested a transcription-independent mechanism for GC in suppressing signaling mediators. Following TLR engagement, recruitment of IL-1R–associated kinase 1 (IRAK1) and TNFR-associated factor 6 (TRAF6) is

*Division of Human Genetics, Cincinnati Children's Hospital Medical Center, University of Cincinnati, Cincinnati, OH 45229; [†]Neonatal Division, International Peace Maternity and Child Health Hospital of China Welfare Institution, School of Medicine, Shanghai Jiao Tong University, Shanghai 200030, People's Republic of China; [‡]Division of Neonatology and Pulmonary Biology, Cincinnati Children's Hospital Medical Center, Cincinnati, OH 45229; [§]Division of Pulmonary Biology, Translational Pulmonary Science Center, Cincinnati Children's Hospital Medical Center, Cincinnati, OH 45229; [¶]Experimental Hematology and Oncology, Cincinnati Children's Hospital Medical Center, Cincinnati, OH 45229; and [‖]Department of Immunology, Southwestern Medical Center, University of Texas, Dallas, TX 75390

ORCIDs: 0000-0003-4926-1319 (Z.L.); 0000-0002-1897-6461 (V.G.J.); 0000-0002-0301-8770 (L.J.M.); 0000-0002-8142-2488 (C.P.).

central in mediating inflammatory reactions. Dysfunction of IRAK1 is associated with several human pathologic entities, including sepsis and inflammation-associated cancer (24–27). Recruitment of IRAK1 to MyD88 forms a MyD88–IRAK1–TRAF6 complex (28) (Supplemental Fig. 1A). Once IRAK1 is phosphorylated (29), this complex is released from MyD88 and forms an IRAK1–TRAF6–TAB–TAK1 complex on the membrane (30). At the membrane, K48 linkage-mediated ubiquitination and degradation/modification of IRAK1 promote trafficking of the TRAF6–TAB–TAK1 complex to the cytosol and subsequent induction of MAPK and NF-κB activation (31, 32). Inhibition of IRAK1 degradation/modification prevents trafficking of the TRAF6–TAK1 complex as well as JNK and IKK phosphorylation (31). IRAK1 also undergoes K63 linkage-specific ubiquitination. Several lines of evidence have indicated that K63-linked IRAK1 ubiquitination facilitates TLR-induced activation of NF-κB (32, 33). Further, Pellino 3b (E3 ligase) –mediated K63-linked ubiquitination competes with K48-linked IRAK1 ubiquitination at the same ubiquitination site, Lys^{134} of IRAK1, and thereby negatively regulates IL-1–induced TAK1-dependent NF-κB activation (34). Together, ubiquitination by various E3 ligases regulates the stability and actions of IRAK1. Although ubiquitination of IRAK1 is pivotal in mediating TNF-α, IL-1, and TLR ligand–mediated inflammation, the ability of GC to regulate IRAK1 ubiquitination has not been determined.

We have developed a unique in vitro model to investigate stimulus-specific GC regulation of IRAK1 ubiquitination by perturbing various TLR ligand–induced IRAK1 ubiquitination and consequential inflammatory actions in macrophages with the synthetic GC dexamethasone (Dex). In this study, we test the hypothesis that GC restrains TLR ligand–induced inflammation via inhibition of IRAK1 ubiquitination. We demonstrated that ligand-specific responsiveness to IRAK1 ubiquitination may account for GC anti-inflammatory efficacy, depending on the inflammatory stimulus.

Materials and Methods

Mice and cell culture

Mice were housed on a 12-h light/12-h dark cycle. Mice used for the experimentation were male, 6–8 wk old, and of C57BL/6 × 129/Sv background. The experimental protocols were approved by the Animal Care and Use Committee of Cincinnati Children's Research Foundation. Mice with conditional deletion of GC receptor (GR) in macrophages (MGRKO) were generated using *LysM* promoter–driven, *Cre* recombinase–mediated excision of exons 1C and 2 of the GR gene (35, 36). Sex-matched *LysM-Cre*–negative homozygous floxed GR littermates were used as controls for the MGRKO mice. Thioglycollate-elicited macrophages were isolated by peritoneal lavage and cultured as described (22). IRAK1$^{-/-}$ immortalized mouse macrophages (IMM) were maintained in DMEM (glucose, 4.5 g/l), 10% FBS, 20 mM HEPES, and 2 mM glutamine, as described (37).

Materials

LPS (LPS-EB Ultrapure, *Escherichia coli* 0111:B4), poly(I:C) (catalog no. Tlrl-pic), CpG oligonucleotide 1826 (5′-TCC ATG ACG TTC CTG ACG TT-3′), and R848 were purchased from InvivoGen (San Diego, CA) and reconstituted per the manufacturer's instructions. Dex, *N*-ethylmaleimide, mifepristone (RU-486) (Sigma-Aldrich, St. Louis, MO), and cycloheximide (CHX; EMD Millipore, Billerica, MA) were purchased and reconstituted per the manufacturers' instructions. Abs used in this study were as follows: anti-actin (A5060) (Sigma-Aldrich); anti-TAK1 (5206, 4505), anti–phospho-SAPK/JNK (4668, 9251), anti-SAPK/JNK (9253, 9252), anti–phospho-p38 MAPK (4511, 9211), anti–p38 MAPK (9211, 9212), anti–phospho-IκBα (2859) and anti-IκBα (4814, 9242), anti-IRAK1 (4504), anti-K63-linked polyubiquitin Ab (5621), anti-MEK1/2 (8727), anti-AIF (5318), anti-PDI (3501), anti-MEKK3 (5727), β-TrCP (4394), normal rabbit IgG control (2729) (Cell Signaling Technology, Beverly, MA); anti-TAK1 (7162), anti-IRAK1 (7883), anti-TRAF6 (7221), anti-GR (1004), anti–phospho-MEKK3 (28044) (Santa Cruz Biotechnology, Santa Cruz, CA); anti–phospho-TAK1 (06-1425), anti-K48-linked polyubiquitin Ab (Apu2,

05-1307), and anti–K63-linked polyubiquitin Ab (Apu3, 05-1308) (Millipore, Temecula, CA); rabbit anti-IgG control (ab465400) (Abcam, Cambridge, MA). For immunoprecipitation experiments, beads used in this study were as follows: protein A (5621) and protein G (8740) magnetic beads (Cell Signaling Technology); and Dynabeads protein A (10002D) Dynabeads protein G (10004D) (Invitrogen, Carlsbad, CA). IRAK1 Ab 7883 was used for the studies that assessed protein–protein interactions between IRAK1 and GR. Experiments that analyzed IRAK1 abundance used IRAK1 Ab 4505.

Human peripheral blood monocyte-derived macrophages

Heparinized blood was obtained by phlebotomy from normal healthy volunteers. PBMCs were isolated by centrifugation on a Ficoll density gradient (density, 1.078 g/ml) (Ficoll-Paque Premium; GE Healthcare Life Sciences), according to the manufacturer's instructions. Cells were washed with PBS and suspended in the cell culture medium (DMEM; Thermo Fisher Scientific, Rockford, IL) with 10% FBS, penicillin (100 U/ml), and streptomycin (100 μg/ml). PBMC suspensions were aliquoted into plastic tissue culture plates and incubated for 2 h at 37°C, 5% CO$_2$ as described previously (38). After removal of nonadherent cells and gentle washing with PBS, the adherent cells (monocytes) were cultured in the presence of recombinant human M-CSF (25 ng/ml; R&D Systems) for 7 d. Differentiated macrophages were washed and cultured for 2 d in serum-free medium for subsequent experiments.

Subcellular fractionation

The cytoplasmic and membrane proteins were extracted by utilizing a subcellular protein fractionation kit (Thermo Scientific). In brief, cytoplasmic extraction buffer containing protease and phosphatase inhibitors was added to 6×10^6 cells, incubated at 4°C for 10 min with gentle mixing, and centrifuged at $500 \times g$ for 5 min. The supernatants (cytoplasmic fraction) were immediately transferred to clean prechilled tubes on ice. In the next step, ice-cold membrane extraction buffer containing protease and phosphatase inhibitors was added to the pellets. The tubes were vortexed for 5 s and incubated at 4°C for 10 min with gentle mixing and centrifuged at $3000 \times g$ for 5 min. The supernatants (membrane fraction) were immediately transferred to clean prechilled tubes on ice. The cytosolic and membrane fractions were analyzed by immunoblot analysis with Abs to the markers MEK1/2 (cytosol), AIF, and PDI (membrane) to determine the purity of the individual fractions.

Immunoprecipitation

Mouse peritoneal macrophages or IRAK1$^{-/-}$ immortalized mouse macrophages were treated with LPS (0.1 μg /ml), CpG (12.5 μg /ml), poly(I:C) (50 μg /ml), or R848 (1 μg/ml) in the presence or absence of 100 nM Dex for the indicated periods of time. Cells were harvested by washing with cold PBS and then lysed with ice-cold protein extraction buffer (PE buffer) that consists of 1% Nonidet P-40 (v/v), 20 mM Tris-HCl (pH 7.5), 2 mM EDTA, 150 mM NaCl, 1 mM DTT, protease inhibitor mixture (P8340; Sigma-Aldrich), phosphatase inhibitor mixture 2 (P5726; Sigma-Aldrich), and phosphatase inhibitor mixture 3 (P0044; Sigma-Aldrich). The lysates were centrifuged at 13,200 rpm for 10 min and insoluble debris was discarded. Two hundred fifty micrograms of the supernatants was incubated with anti-IRAK1 or anti-GR Ab and magnetic Sepharose beads in immunoprecipitation buffer (IP buffer) per the manufacturer's instruction. The precipitates were resolved by SDS-PAGE and subjected to immunoblot analysis with the indicated Abs.

Immunoblot analysis

Whole-cell, cytoplasmic, and membrane extracts were resolved through SDS-PAGE using 4–12% separating gel (Invitrogen). Proteins were transferred to Hybond ECL nitrocellulose membrane (Amersham Pharmacia Biotech, Piscataway, NJ) using a semidry transfer system (Bio-Rad, Hercules, CA) and blocked with 5% dried milk in PBS and 0.1% Tween 20 (Sigma-Aldrich). Blots were probed with primary Ab overnight at 4°C. Binding of HRP-labeled goat anti-rabbit Ab (sc-2004) or goat anti-mouse Ab (sc-2005) (Santa Cruz Biotechnology) was determined using Super-Signal West chemiluminescent substrate (Thermo Scientific). Blots were stripped with Restore Western blot stripping buffer (Thermo Scientific) and reprobed with different Abs.

Ubiquitination assays

Cells were harvested by washing with ice-cold PBS and then lysed in buffer containing 1% SDS, 20 mM Tris-HCl (pH 7.5), 2 mM EDTA, 150 mM NaCl, 1 mM DTT, protease inhibitor mixture, phosphatase inhibitor mixture, and 20 mM *N*-ethylmaleimide.

The whole-cell lysates (WCL) were centrifuged at 13,200 rpm for 10 min and insoluble debris was discarded. Two hundred fifty micrograms of the supernatants was incubated with anti-IRAK1 and magnetic Sepharose beads in immunoprecipitation buffer containing 0.1% SDS (per the manufacturer's instructions). The precipitates were resolved by SDS-PAGE and subjected to immunoblot analyses with Abs against anti-K63 or anti-K48 linkage-specific polyubiquitin Ab.

In vivo treatment with TLR ligands and Dex

LPS, CpG, and Dex were reconstituted in sterile endotoxin-free physiological water (NaCl 0.9%) (InvivoGen). Male mice of 6–8 wk of age were injected with LPS (5 mg/kg) or CpG (5 mg/kg) i.p. To examine GC effect on TLR ligand–mediated inflammatory actions, Dex (10 mg/kg) was coinjected with LPS or CpG. Blood was collected after the indicated periods of treatments by retro-orbital phlebotomy into heparinized capillary tubes, with the time from first handling the animal to completion of the bleeding not exceeding 30 s. Plasma samples were stored at −80°C until assay. Proinflammatory cytokine concentrations in plasma samples were measured by ELISA for TNF-α and IL-6 per the manufacturer's instructions (BD Biosciences/BD Pharmingen, San Diego, CA).

Ex vivo ubiquitination assays

Following in vivo treatments with TLR ligands and Dex (as described in the above section), resident peritoneal macrophages were isolated by peritoneal lavage. Macrophages were purified by attachment to the tissue culture plate for 2 h. Following attachment, cells were immediately harvested for ubiquitination assays.

Transfection

IRAK1 ubiquitination mutants were engineered by site-directed mutagenesis as described previously. RAW 264.7 cells were transfected with different amounts of empty pCMV vector or vector containing the Lys[134] mutant plasmid (IRAK1 ubiquitination mutant, K134R) (a gift from Dr. X. Li, Cleveland Clinic, Cleveland, OH) for 24, 48, and 72 h. Transfection of the indicated plasmids by Lipofectamine 3000 transfection reagents was done as recommended by the manufacturer (Thermo Fischer Scientific).

In vitro cytokine measurement

Cells were plated at 10^6 cells/ml in 24-well plates (Becton Dickinson Labware, Franklin Lakes, NJ) with 1 ml of complete medium. Cells were cotreated with Dex and LPS or CpG for 18 h in the presence or absence of empty vector or vector containing K134R plasmid. Supernatants were collected and cytokine concentrations were measured by ELISA for TNF-α, IL-6, and IL-12 (BD Biosciences/BD Pharmingen).

Statistical analysis

All experiments were replicated two to three times to assure the reproducibility of the observations. Statistical analysis was performed with GraphPad Prism software v6. Data were tested for normality (Kolmogorov–Smirnov test). Results that passed the normality assumption were analyzed by an unpaired two-tailed Student t test. Data that failed the normality assumption were analyzed by the nonparametric Mann–Whitney U test with post hoc analysis. Data were expressed as the mean ± SD. Differences were considered statistically significant for p values < 0.05.

Results

GC suppression of TLR ligand–induced inflammatory signals requires the inhibition of posttranscriptional modification of signal transducers

We previously reported inefficient GC suppression of both inflammatory cytokines and key signaling intermediates that are induced or activated following LPS treatment as compared with treatment with CpG or poly(I:C) (Supplemental Fig. 1B) (21). In these studies, mouse peritoneal macrophages were pretreated with Dex for 3 h before the challenge with TLR ligands. In this study, we examined whether Dex suppression of inflammatory reactions requires inhibition of new translation that could occur within the 3 h of Dex pretreatment. We compared TLR ligand–induced phosphorylation of TAK1, IκBα, JNK, and p38 MAPK in cells that were pretreated with Dex or cotreated with Dex in the presence of TLR ligands. In LPS-treated cells, pretreatment or cotreatment

with Dex did not inhibit the phosphorylation of TAK1, IκBα, JNK, or degradation of IκBα (Fig. 1A). Only p38 MAPK phosphorylation was found to be Dex suppressible. Pretreatment or cotreatment with Dex resulted in comparable inhibition of LPS-mediated p38 MAPK phosphorylation. In poly(I:C)-treated cells, pretreatment with Dex resulted in more robust inhibition of TAK1, JNK, and p38 MAPK phosphorylation, compared with cotreatment with Dex (Fig. 1A, Supplemental Table I). After the treatment with poly(I:C), only modest phosphorylation and degradation of IκBα was observed, which was unaltered by pre- or cotreatment with Dex (Fig. 1A). In CpG-treated cells, pretreatment with Dex resulted in similar inhibition of TAK1, IκBα, JNK, and p38 MAPK phosphorylation, compared with cotreatment with Dex (Fig. 1A, Supplemental Table I).

Based on Dex inhibition of CpG- and LPS-induced phosphorylation of signaling mediators within minutes of cotreatment, we anticipated that Dex-mediated suppression might not require new translation. To test this hypothesis, cells were pretreated with CHX for 45 min, followed by treatment with Dex for 3 h, and finally with individual TLR ligand for 30 min. We detected comparable reduction in LPS-induced p38 MAPK phosphorylation in Dex-pretreated cells in the absence and presence of CHX, respectively (Fig. 1B, Supplemental Table II). In CpG-treated cells, similar inhibition of TAK1, IκBα, JNK, and p38 MAPK phosphorylation was detected in the Dex only treatment group, compared with the Dex plus CHX treatment group (Fig. 1B, Supplemental Table II). In these experiments, we observed only modest CHX-dependent reversal of GC-mediated inhibition of TAK1 and IκBα phosphorylation but no JNK phosphorylation. Data in this study suggest that GC suppression of CpG-induced inflammatory reactions are predominantly independent of new protein synthesis. In poly(I:C)-treated cells, inhibition of TAK1, JNK, and p38 MAPK phosphorylation in the Dex only treatment group was more pronounced than in the Dex plus CHX treatment group (Fig. 1B, Supplemental Table II). Notably, pretreatment with Dex for 3 h inhibited poly(I:C)-induced phosphorylation of signaling intermediates, whereas cotreatment with Dex plus poly(I:C) had no inhibitory effect (Fig. 1A). Results from the experiments with CHX are consistent with the temporal pattern of Dex suppression of poly(I:C)-mediated TAK1, JNK, and p38 MAPK activation in the cotreatment experiments. Whereas Dex inhibits poly(I:C)-mediated activation of TAK1, JNK, and p38 MAPK, most Dex suppression is likely due to substantial regulation of genomic actions and require new translation. Based on this evidence for new translation-independent GC regulation of inflammatory signaling mediators, all subsequent experiments to examine GC effects on TLR4 and TLR9 ligand–induced inflammation were performed by cotreatment with Dex and the relevant TLR ligand.

GC inhibits TLR ligand–induced K48-linked ubiquitination and degradation/modification of IRAK1

IRAK1 functions as an upstream signaling mediator for both NF-κB and MAPK activation. IRAK1 ubiquitination, a posttranscriptional modification, is required for its activation. Therefore, we investigated Dex effects on ligand-induced IRAK1 ubiquitination. In these experiments, cells were cotreated with Dex and individual TLR ligands. IRAK1 was immunoprecipitated in the WCL with an anti-IRAK1 Ab or isotype-matched control IgG, followed by immunoblotting with anti-ubiquitin K48 linkage–specific Ab. K48-linked ubiquitination of IRAK1 in rested cells was detectable at a very low abundance with or without treatment with Dex (Fig. 2A). Treatment with LPS resulted in marked elevation of K48-linked IRAK1 ubiquitination as early as 5 min after
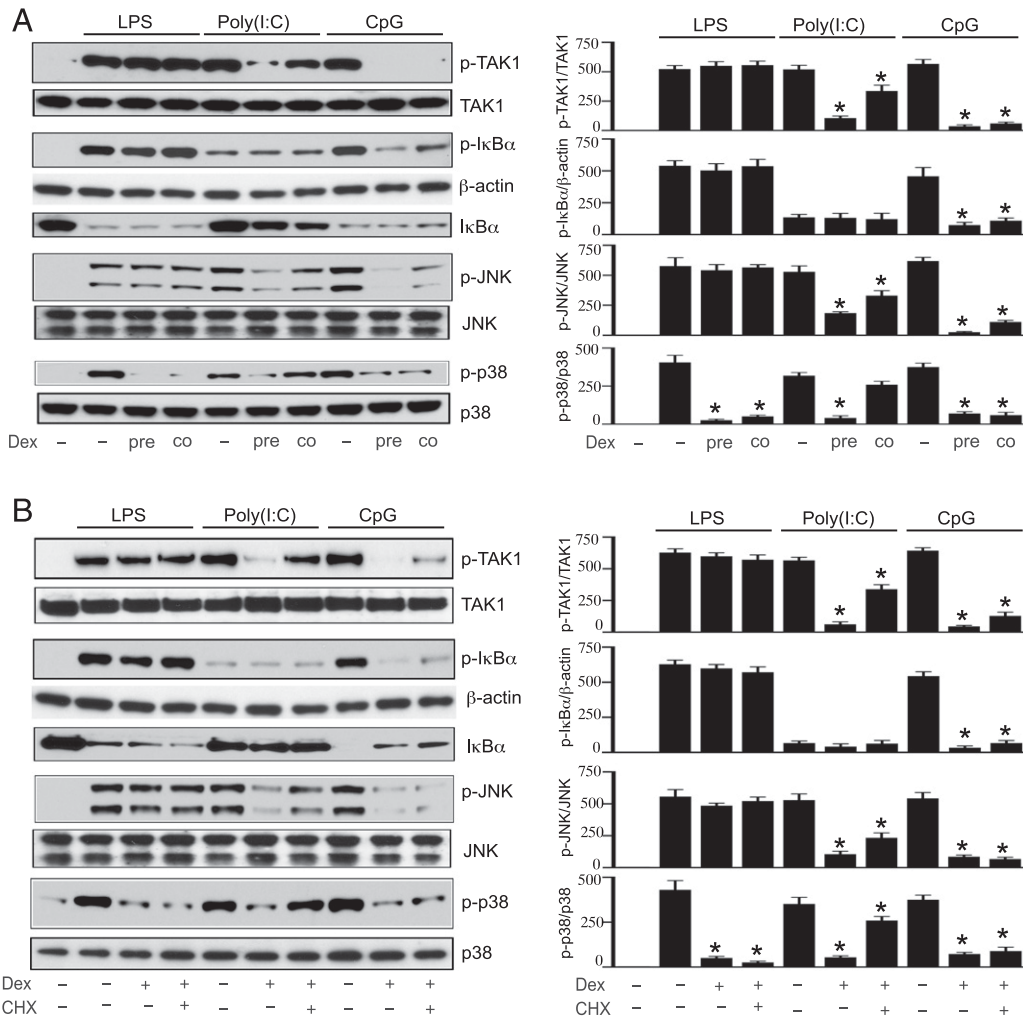
FIGURE 1. Dex suppresses inflammatory signals via inhibition of posttranslational modifications of signaling mediators. (**A**) Effect of pretreatment (pre) versus cotreatment (co) with Dex on TLR ligand–mediated activation of inflammatory signals. Mouse peritoneal macrophages were pretreated (pre) with 100 nM of Dex for 3 h, followed by treatment with LPS (0.1 μg/ml), CpG (12.5 μg/ml), or poly(I:C) (50 μg/ml) for 30 min. In another set of experiments, cells were cotreated with Dex and individual TLR ligand for 30 min. (**B**) Effect of CHX treatment on Dex suppression of inflammatory signals. Macrophages were treated with 10 μM CHX for 45 min, followed by treatment with Dex for 3 h and subsequently with the individual TLR ligand for 30 min. WCL were analyzed by Western blot using anti–phospho-TAK1 (p-TAK1), total TAK1; anti–phospho-IκBα (p-IκBα), total IκBα; anti–phospho JNK (p-JNK), total JNK; anti–phospho p38 MAPK (p-p38) and total p38 MAPK (p38) Abs. Western blots were quantified by densitometric analyses. Abundance of phosphorylated proteins were normalized to total protein or β-actin, as appropriate. Protein expression in untreated, resting cells were considered as 1 U. The densitometry data presented are mean ± SD. Western blots are from a single experiment that are representative of three to four independent experiments. *$p < 0.05$ versus cells treated with respective TLR ligand.

ligand treatment. We observed persistent ubiquitination until 30 min after LPS challenge, with a sharp decline after 60 min of LPS treatment. Treatment with Dex had no effect on LPS-mediated K48-linked IRAK1 ubiquitination. In poly(I:C)-treated cells, only modest levels of K48-linked IRAK1 ubiquitination were observed and not altered by Dex exposure (Fig. 2B). Within 15 min of treatment with CpG, we found robust K48-linked IRAK1 ubiquitination that was further enhanced after 30 min of treatment (Fig. 2C). The relatively early induction of LPS-mediated IRAK1 ubiquitination could be due to more robust inflammatory reactions at the downstream of TLR4 engagement that promotes the recruitment of both MyD88 and Toll/IL-1R domain–containing adapter inducing IFN-β (Trif) as compared with only MyD88-dependent actions following TLR9 engagement. Exposure to Dex resulted in 2- and 9-fold inhibition of IRAK1 ubiquitination after 15 and 30 min of CpG treatment, respectively (Fig. 2C). After 60 min of CpG treatment IRAK1 ubiquitination was undetectable, whereas a low level of ubiquitinated IRAK1 was ob-

served in Dex-exposed cells. To examine Dex specificity for the GR pathway, we repeated the experiments with mifepristone (RU-486), a GR antagonist. In the presence of RU-486, CpG treatment–induced K48-linked IRAK1 ubiquitination was not Dex suppressible (Fig. 2D). Therefore, Dex inhibition of K48 linkage–specific IRAK1 ubiquitination is mediated via GR. To assess whether Dex inhibited TLR ligand–induced IRAK1 ubiquitination in human macrophages, K48-linked IRAK1 ubiquitination was evaluated in immortalized human macrophages (THP-1 cells). Treatment of THP-1 cells with Dex inhibited CpG-induced K48-linked IRAK1 ubiquitination by 8-fold ($p = 0.002$); however, Dex had no effect on LPS-induced K48-linked IRAK1 ubiquitination (Fig. 2E).

We evaluated GC sensitivity for TLR-mediated IRAK1 ubiquitination in human monocyte-derived primary macrophages. TLR7, TLR8, and TLR9 have closely related molecular structures (39, 40), and they mediate comparable immune responses when recognizing nucleic acid ligands (41). These endosomal TLRs
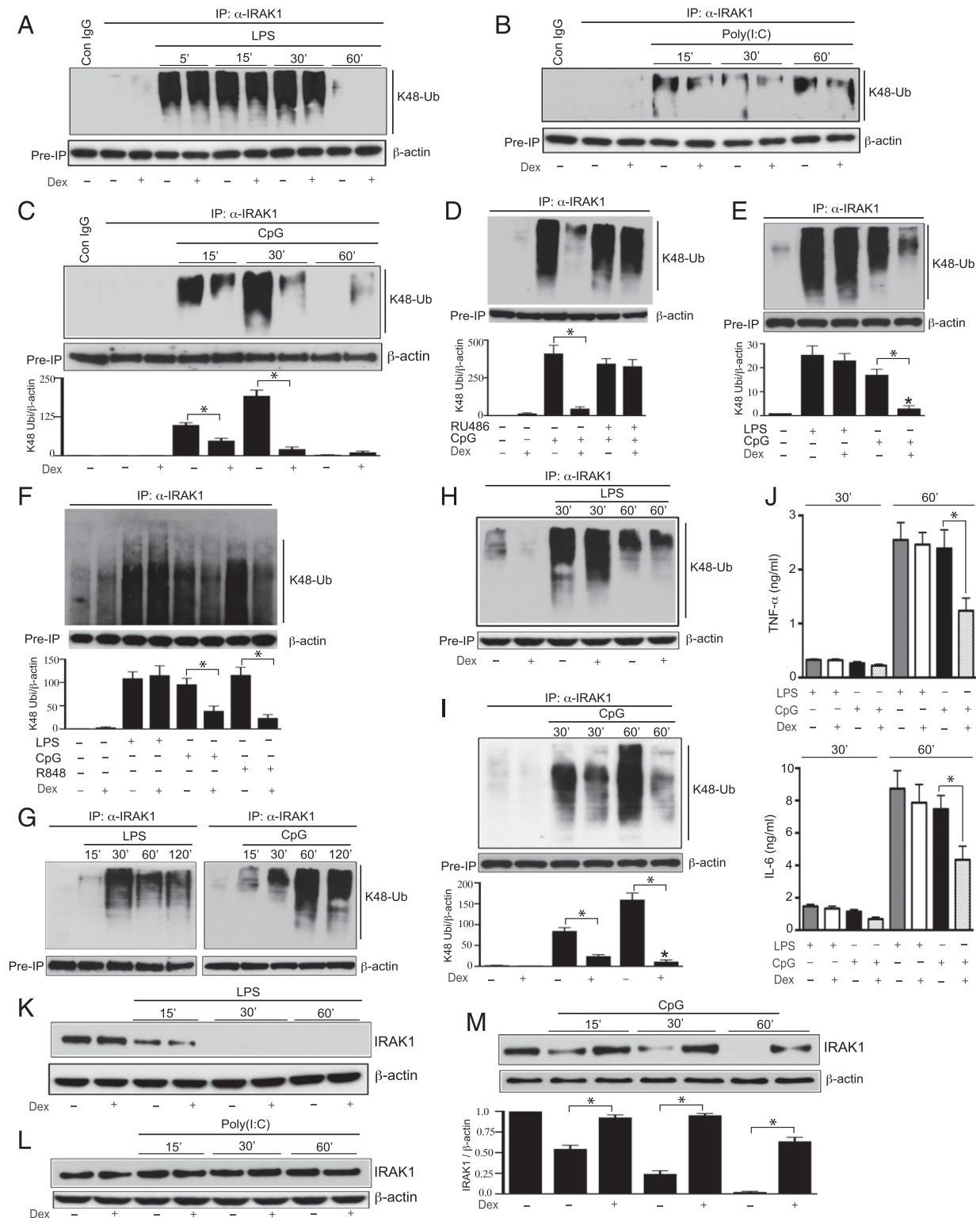
FIGURE 2. Effect of Dex on TLR ligand–mediated K48-linked ubiquitination and degradation of IRAK1. Peritoneal mouse macrophages were treated with (**A**) LPS, (**B**) poly(I:C), and (**C**) CpG with or without Dex for the indicated periods of time. Dex was cotreated with the TLR ligands. (**D**) Peritoneal mouse macrophages were pretreated with RU-486 (1 μM) for 1 h, followed by cotreatment with CpG and Dex for 30 min. (**E**) THP-1 cells were treated with LPS or CpG in the presence or absence of Dex for 30 min. (**F**) Human monocyte-derived macrophages were treated with LPS (0.1 μg/ml), CpG (12.5 μg/ml), or R848 (1 μg/ml) in the presence or absence of Dex for 30 min. (**G**) Male mice (*n* = 4–6 per group) were injected i.p. with LPS (5 mg/kg) or CpG (5 mg/kg) for the indicated periods of time. Resident peritoneal macrophages were harvested for ex vivo ubiquitination assays. (**H** and **I**) Male mice (*n* = 5–6 per group) were cotreated with Dex (10 mg/kg) and (H) LPS (5 mg/kg) or (I) CpG (5 mg/kg) for the indicated periods of time. Resident peritoneal macrophages were harvested for ex vivo ubiquitination assays. WCL were immunoprecipitated with anti-IRAK1 Ab, followed by immunoblotting with anti-ubiquitin K48 linkage–specific Ab. (**J**) Plasma samples were collected from the experiments as described for (H) and (I). Concentrations of TNF-α and IL-6 were analyzed by ELISA. Data are presented as mean ± SEM. *$p < 0.05$ versus mice cotreated with Dex and CpG. (**K–M**) In similar experiments [as described for (A)–(C)], WCL were analyzed by immunoblotting with anti-IRAK1 and anti–β-actin Abs. Western blots were quantified by densitometric analyses. (C–F and I) The abundance of K48 linkage–specific IRAK1 ubiquitination was normalized to β-actin. IRAK1 ubiquitination in untreated, *(Figure legend continues)*

detect nucleic acids and engage MyD88 as the common mediator of inflammatory pathways (42). Notably, TLR7 and TLR8 are abundantly expressed in human macrophages, whereas expression of TLR9 is relatively low. Treatment of human macrophages with TLR4 or TLR7/8 ligand induced K48-linked IRAK1 ubiquitination more prominently than did treatment with TLR9 ligand (Fig. 2F). Cotreatment with Dex did not inhibit TLR4-induced K48-linked IRAK1 ubiquitination. However, exposure to Dex suppressed TLR9 or TLR7/8 ligand–mediated K48-linked IRAK1 ubiquitination by 2- and 5-fold, respectively. Therefore, GC adopts similar regulation of K48 linkage–specific IRAK1 ubiquitination induced by TLR7/8 or TLR9 ligand in human macrophages.

Next, we analyzed GC regulation of IRAK1 ubiquitination in vivo. Intraperitoneal injection of male mice with LPS or CpG resulted in marked elevation of K48-linked IRAK1 ubiquitination in resident peritoneal macrophages, although the kinetics were somewhat different. These differences were likely due to the absorption and distribution of TLR ligands and Dex following i.p. injections. The maximum level of IRAK1 ubiquitination was observed after 30 and 60 min of treatment with LPS and CpG, respectively (Fig. 2G). There was no detectable inhibition of LPS-mediated K48-linked IRAK1 ubiquitination in Dex-treated animals (Fig. 2H). In contrast, after 30 and 60 min of treatment with CpG, 3.5- and 14.5-fold inhibition of K48-linked IRAK1 ubiquitination was observed in Dex-treated animals (Fig. 2I). Hence, both in vitro and in vivo Dex suppressed CpG but not LPS-mediated K48-linked IRAK1 ubiquitination. Also, compared with CpG only–treated mice, cotreatment with Dex and CpG resulted in a 48 and 42% reduction in plasma concentration of TNF-α ($p = 0.037$, $n = 5$–6) and IL-6 ($p = 0.04$, $n = 6$) after 60 min of CpG treatment (Fig. 2J). However, Dex had no significant effect on LPS-induced elevated plasma levels of TNF-α or IL-6.

Because K48-linked ubiquitination initiates the degradation/modification of IRAK1, we examined the effect of Dex treatment on IRAK1 abundance. Treatment with poly(I:C) did not promote degradation/modification of IRAK1 (Fig. 2L). This is consistent with the negligible amount of K48-linked IRAK1 ubiquitination induced by poly(I:C) (Fig. 2B). Within 15 min of LPS treatment, reduction in IRAK1 abundance was observed compared with the untreated cells; after 30 min of LPS challenge, IRAK1 abundance was undetectable (Fig. 2H). This disappearance of IRAK1 can be due to IRAK1 modification or degradation as previously reported by two independent studies (32, 43). Nevertheless, exposure to Dex had no effect on LPS-mediated reduction of IRAK1 abundance. In contrast, Dex prevented CpG-induced reduction of IRAK1 abundance (Fig. 2M). β-Actin was used as a preimmunoprecipitated loading control in these experiments due to IRAK1 degradation/modification in response to LPS or CpG treatment. Taken together, these results suggest strong Dex sensitivity for CpG-induced K48-linked IRAK1 ubiquitination both in vitro and in vivo.

GC inhibition of the trafficking of IRAK1 and IRAK1-interacting partners

K48-linked ubiquitination of IRAK1 facilitates membrane-to-cytoplasm trafficking of the TRAF6–TAK1 complex, and it was suggested to be involved in the activation of TAK1 and NF-κB (31). In unstimulated cells, TRAF6, TAK1, and IRAK1 were predominantly present in the cytoplasm and modestly represented within the membrane fraction (Fig. 3A, 3C, 3E). After 10 min of treatment with CpG or LPS, TRAF6 and TAK1 translocated from the cytoplasm to the cell membrane. This translocation is followed by subsequent repositioning of TRAF6 and TAK1 to the cytoplasm within 20 min of ligand challenges (Fig. 3A–D). We determined the effect of GC regulation on the intracellular trafficking of TRAF6 and TAK1 by evaluating time-dependent abundance of these proteins in cytoplasmic and membrane fractions. To examine the effect of GC on TRAF6–TAK1 trafficking, cells were cotreated with Dex and TLR ligands. There was no effect of Dex treatment on LPS- or CpG-induced TRAF6 and TAK1 translocation to the membrane fraction (Fig. 3A–D). Also, Dex exposure did not alter LPS-mediated trafficking of TRAF6 or TAK1 from the membrane to the cytoplasm (Fig. 3A, 3C). However, in CpG-challenged cells, treatment with Dex resulted in substantial inhibition of TRAF6 and TAK1 trafficking to the cytoplasm (Fig. 3B, 3D). We detected repositioning of TRAF6 from the cytoplasm to membrane after prolonged treatment with LPS or CpG. At present, we do not have a mechanism to explain this phenomenon. We anticipate this could be due to accumulation of TRAF6 following continuous exposure to TLR ligand.

Within 10 min of CpG treatment, a decreased abundance of IRAK1 was observed in the cytoplasm. The kinetics for membrane-to-cytoplasm translocation of IRAK1 was different from TRAF6 or TAK1. After 30 min of CpG treatment we detected cytoplasmic TRAF6 or TAK1, whereas IRAK1 was undetectable. This is likely due to β-TrCP (an E3 ligase)–facilitated K48-linked ubiquitination and subsequent degradation of IRAK1. We found a 4- and 9-fold increase in membrane abundance of IRAK1 after 20 and 30 min of CpG challenge compared with unstimulated cells (Fig. 3E). After 10 and 20 min of CpG challenge the abundance of IRAK1 in the cytoplasm of Dex-treated cells was increased by 3- and 7-fold, respectively, compared with CpG only–treated cells. IRAK1 was undetectable in the cytoplasm after 30 min of CpG treatment in the presence or in the absence of Dex. Following 10, 20, and 30 min of CpG treatment, the abundance of IRAK1 in the membrane of Dex-treated cells was increased by 18-, 10-, and 12-fold, respectively, compared with CpG only–treated cells (Fig. 3E).

Therefore, treatment with Dex enhances membrane retention of TRAF6 and TAK1 and thereby prevents the membrane to cytoplasm trafficking of the protein complex. We did not find detectable change in MEK1/2 (cytoplasmic marker) or AIF (membrane marker) expression among different treatment groups compared with untreated cells. Because Dex had no effect on LPS-induced K48-linked IRAK1 ubiquitination, degradation/modification, or TRAF6-TAK1 trafficking, we did not assess IRAK1 abundance in subcellular fractions of LPS-treated cells.

CpG-induced K48 linkage–mediated ubiquitination and degradation/modification of IRAK1 require ubiquitination at Lys^{134}

Previous studies indicated that a point mutation in IRAK1 at Lys^{134} to Arg abolished IL-1β–induced global IRAK1 ubiquitination and degradation in HeLa cells (43). In this study, we examined the role of ubiquitination at Lys^{134} in mediating CpG-induced K48 ubiquitination and degradation/modification of IRAK1. In these experiments, IRAK1$^{-/-}$ IMM were transfected with varying amounts

resting cells was considered as 1 U. (M) The abundance of IRAK1 was normalized to β-actin. IRAK1 abundance in untreated, resting cells was considered as 1 U. The densitometry data presented are mean ± SD. All Western blots are from a single experiment and are representative of three independent experiments. *$p < 0.05$ versus cells treated with CpG.
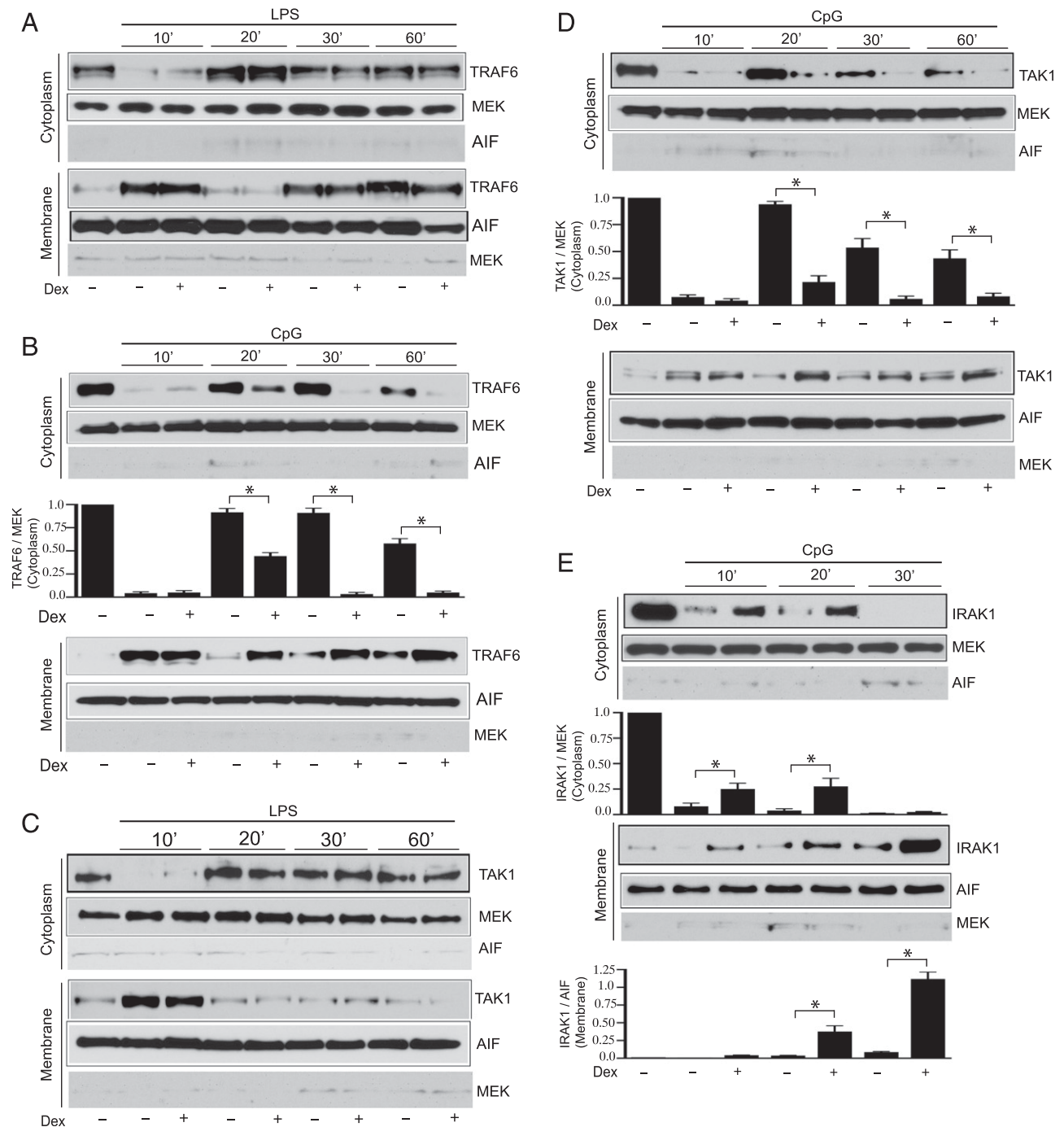
FIGURE 3. Effect of Dex on TLR ligand–induced trafficking of IRAK1 and IRAK1- interacting partners. Peritoneal mouse macrophages were treated with (**A** and **C**) LPS and (**B**, **D**, and **E**) CpG with or without Dex for the indicated periods of time. Dex was cotreated with the TLR ligands. The cytoplasmic and membrane fractions were analyzed by immunoblotting with anti-TRAF6, anti-MEK, anti-AIF and anti-TAK1 and anti-IRAK1 Abs. Western blots were quantified by densitometric analyses. The abundance of TRAF6, TAK1, and IRAK1 was normalized to MEK or AIF, as appropriate. TRAF6, TAK1, and IRAK1 abundance in untreated, resting cells was considered as 1 U. The densitometry data presented are mean ± SD. Western blots are from a single experiment, representative of three to four independent experiments. *$p < 0.05$ versus cells treated with CpG.

of wild-type (WT) or Lys[134] mutant IRAK1 (K134R) plasmid DNA. Transfection of IRAK1$^{-/-}$ IMM with 1000 ng of WT or K134R IRAK1 DNA for 48 h resulted in substantial induction of IRAK1 expression (Fig. 4A). Next, we assessed the requirement of Lys[134] in mediating CpG-induced K48 linkage–specific IRAK1 ubiquitination. Transfection of IRAK1$^{-/-}$ IMM with WT IRAK1 rapidly induced K48 linkage–specific IRAK1 ubiquitination within 15 min of CpG treatment (Fig. 4B), which was also observed in mouse peritoneal macrophages isolated from WT mice harboring

IRAK1 (Fig. 2C). After 15 and 30 min of CpG treatment, we observed 8- and 50-fold inhibition of K48 linkage–specific IRAK1 ubiquitination in IRAK1$^{-/-}$ IMM transfected with K134R mutant IRAK1 (Fig. 4B). Consistent with the data from mouse peritoneal macrophages (Fig. 2C), K48-linked IRAK1 ubiquitination was markedly reduced after 60 min of CpG treatment in IRAK1$^{-/-}$ IMM transfected with WT IRAK1. We also examined whether Dex targets IRAK1 ubiquitination at Lys[134] to inhibit CpG-induced IRAK1 degradation/modification as demonstrated in Fig. 2J. In

these studies, IRAK1$^{-/-}$ IMM transfected with WT or mutant K134R IRAK1 were treated with CpG, with or without Dex (cotreated). To ensure degradation/modification of IRAK1, cells were treated with CpG for 60 min. Treatment with CpG abrogated IRAK1 abundance in WT IRAK1-transfected cells. However, cotreatment with Dex restored IRAK1 abundance (Fig. 4C). Notably, CpG failed to degrade IRAK1 in mutant K134R IRAK1-transfected IRAK1$^{-/-}$ IMM. We found comparable abundance of IRAK1 in Dex plus WT IRAK1 and K134R IRAK1 (only) treatment groups (Fig. 4C). Also, cotreatment of mutant K134R IRAK1-transfected IRAK1$^{-/-}$ IMM treated with CpG and Dex did not have any additional effect on IRAK1 abundance.

GC targets IRAK1 ubiquitination in restraining TLR ligand–induced inflammatory actions

First, we determined the role of Lys^{134} on IRAK1 in mediating CpG- or LPS-mediated K48 linkage–specific ubiquitination. Transfection of IRAK1$^{-/-}$ IMM with WT IRAK1 markedly elevated K48 linkage–specific ubiquitination after treatment with CpG or LPS (Fig. 5A, 5B). Similar to mouse peritoneal macrophages, induction of K48-linked IRAK1 ubiquitination was Dex suppressible following treatment with CpG but not LPS. Treatment of WT IRAK1-transfected IRAK1$^{-/-}$ IMM with Dex resulted in comparable inhibition of K48-linked IRAK1 ubiquitination as did transfection with mutant K134R IRAK1 (without Dex) (Fig. 5A). We observed 6.6- and 5-fold inhibition of Dex and K134R IRAK1-mediated K48-linked IRAK1 ubiquitination, respectively, compared with CpG-induced ubiquitination in WT IRAK1-transfected IRAK1$^{-/-}$ IMM. Cotreatment of K134R IRAK1-transfected IRAK1$^{-/-}$ IMM with Dex and CpG did not result in additional inhibition of K48-linked IRAK1 ubiquitination.

Similar experiments to investigate GC inhibition of IRAK1 ubiquitination at Lys^{134} in suppressing inflammatory signaling intermediates indicated inhibition of CpG-induced TAK1, IκBα, JNK, and p38 MAPK phosphorylation in K134R-transfected cells. In WT IRAK1-transfected IRAK1$^{-/-}$ IMM, Dex inhibited the phosphorylation of IκBα, JNK, and p38 MAPK, as expected (Fig. 5C). With no Dex exposure, we observed 7-, 3-, 3-, and 8-fold inhibition of TAK1, IκBα, JNK, and p38 MAPK phosphorylation, respectively, in K134R-transfected and CpG-treated cells as compared with WT IRAK1-transfected cells (Fig. 5C). A similar experiment with Dex treatment of WT IRAK1-transfected IMM indicated 5-, 15-, 4-, and 4-fold inhibition of TAK1, IκBα, JNK, and p38 MAPK phosphorylation compared with WT IRAK1-transfected IMM (Fig. 5C). Thus, ablation of IRAK1 ubiquitination at Lys^{134} showed comparable inhibition of the activation of inflammatory signal mediators, as did treatment with Dex.

The biological relevance of IRAK1 ubiquitination at Lys^{134} is not known. We examined whether GC modulation of IRAK1 ubiquitination at Lys^{134} accounts for suppression of proinflammatory cytokine synthesis/secretion in IMM. In WT IRAK1-transfected IRAK1$^{-/-}$ IMM, exposure to Dex resulted in a 47, 59, and 51% inhibition of IL-6, TNF-α, and IL-12 secretion induced by CpG (Fig. 5D, Supplemental Table III). Transfection of IRAK1$^{-/-}$ IMM with mutant K134R IRAK1 (without Dex) suppressed CpG-mediated secretion of IL-6, TNF-α, and IL-12 by 39, 53, and 35%, respectively (Fig. 5D, Supplemental Table III). Notably, cotreatment of IRAK1$^{-/-}$ IMM with Dex and K134R IRAK1 plasmid did not cause additional suppression of proinflammatory cytokines. Taken together, these results suggest that Dex suppression of CpG-induced inflammatory mediators is primarily mediated by defective IRAK1 ubiquitination at Lys^{134}.

In LPS-treated and WT IRAK1-transfected IRAK1$^{-/-}$ IMM, Dex exposure inhibited IL-6, TNF-α, and IL-12 secretion by 50,

48, and 63% compared with LPS only–treated cells (Fig. 5E, Supplemental Table III). Transfection of IRAK1$^{-/-}$ IMM with K134R IRAK1 inhibited LPS-induced IL-6, TNF-α, and IL-12 secretion by only 17, 18, and 26%, respectively, compared with WT IRAK1-transfected IRAK1$^{-/-}$ IMM (Fig. 5E, Supplemental Table III). However, exposure of K134R-transfected IRAK1$^{-/-}$ IMM to Dex resulted in a significant additional suppression of LPS-mediated cytokine secretion. Treatment with Dex resulted in 83, 90, and 97% inhibition of LPS-induced IL-6, TNF-α, and IL-12 secretion compared with LPS only–treated cells (Fig. 5E, Supplemental Table III). Thus, Dex suppression of LPS-mediated inflammatory responses does not require inhibition of IRAK1 ubiquitination at Lys^{134}.

Direct protein–protein interactions between GR and IRAK1

GC-mediated suppression of CpG-induced IRAK1 ubiquitination and trafficking of TRAF6 or TAK1 occurred within minutes of ligand challenge. We examined whether there is any direct interaction between IRAK1 and GR. In coimmunoprecipitation studies, GR was immunoprecipitated and then immunoblotted with an anti-IRAK1 Ab. There was no detectable protein–protein interaction between IRAK1 and GR, when the cells were treated with LPS with or without Dex (Fig. 6A). Following treatment with CpG, we observed only moderate protein–protein interaction between GR and IRAK1 that prominently increased in the presence of Dex. After 10, 15. and 20 min of CpG treatment, there was a 10-, 5-, and 30-fold increase in GR–IRAK1 interaction after Dex treatment compared with the cells that were not treated with Dex (Fig. 6B). GR interacted with IRAK1 of a higher molecular mass (∼100 kDa) than the unmodified form (∼78 kDa) in the preimmunoprecipitated WCL.

Next, we assessed the nature of IRAK1 modifications required for direct physical interaction between IRAK1 and GR. Notably, Lys^{134} on IRAK1 is a common motif for both K48- and K63-linked IRAK1 ubiquitination (31–33). Our previous findings indicated Dex prevents K48-linked (Fig. 2C) but not K63-linked (Fig. 5F) IRAK1 ubiquitination induced by CpG treatment. We examined whether CpG-induced IRAK1 ubiquitination at Lys^{134} is required for GR–IRAK1 interaction. Consistent with the results from mouse peritoneal macrophages, exposure to Dex substantially enhanced GR–IRAK1 interaction in IRAK1$^{-/-}$ IMM transfected with WT IRAK1 (Fig. 6C). Treatment with Dex plus CpG resulted in a 7-fold increase in GR–IRAK1 interaction compared with CpG only–treated cells. Intriguingly, transfection with mutant K134R IRAK1 suppressed Dex-mediated GR–IRAK1 interaction. There was a 6-fold decrease in GR–IRAK1 interaction in K134R IRAK1-transfected IRAK1$^{-/-}$ IMM, compared with WT IRAK1-transfected IRAK1$^{-/-}$ IMM (Fig. 6C). Our data suggest that IRAK1 ubiquitination at Lys^{134} is required for subsequent protein–protein interactions between GR and IRAK1. These results were unexpected because we found GC inhibition of K48-linked IRAK1 ubiquitination. Notably, Lys^{134} on IRAK1 provides a motif for both K48 and K63 linkage–specific IRAK1 ubiquitination (31–33). Consistently, transfection of IRAK1$^{-/-}$ IMM with mutant K134R IRAK1 strongly suppressed CpG-induced K63-linked IRAK1 ubiquitination (Fig. 6D). It is plausible that K63-linked IRAK1 ubiquitination at Lys^{134} is required for GR–IRAK1 interactions, however not GC suppressible. We examined GC effects on CpG-induced K63-linked IRAK1 ubiquitination. In mouse peritoneal macrophages, K63 linkage–specific IRAK1 ubiquitination was detectable within 5 min of CpG treatment and persisted for 20 min after CpG challenge (Fig. 6E). Dex had no inhibitory effect on CpG-mediated K63-linked IRAK1 ubiquitination.
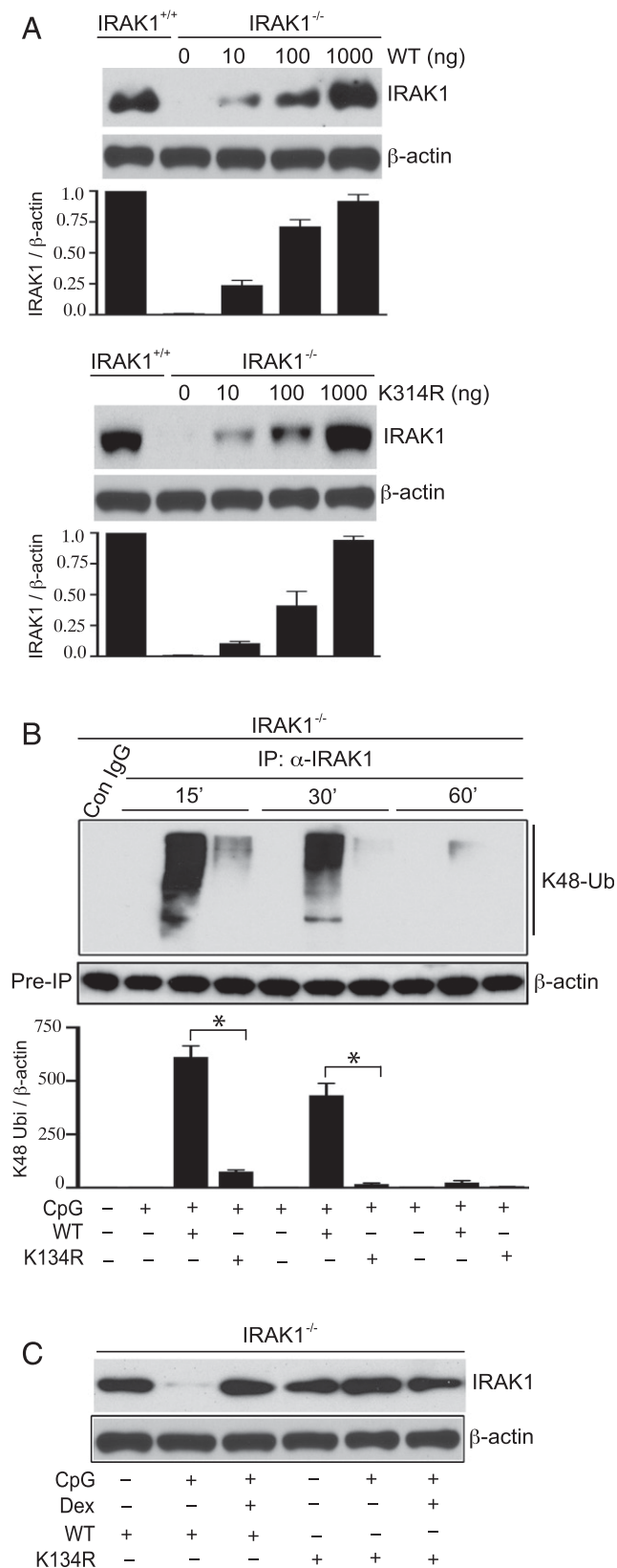
β-TrCP, an E3 ligase, physically interacts with IRAK1 and facilitates K48-linked ubiquitination of IRAK1 (31). We sought to determine whether the Dex-mediated direct physical interaction between GR and IRAK1 interferes with β-TrCP–IRAK1 interactions. There was no detectable protein–protein interaction between IRAK1 and β-TrCP in the nontreated cells. However, treatment with CpG markedly enhanced direct protein–protein interaction between IRAK1 and β-TrCP (Fig. 6F). Following 10 and 20 min of CpG treatment, there was a 7- and 34-fold inhibition in IRAK1–β-TrCP interaction in Dex-exposed cells compared with untreated cells (Fig. 6F). Similar experiments were performed with GR-deficient macrophages (GRko) to determine the contribution of GR in preventing interactions between IRAK1 and β-TrCP. In the presence of Dex, protein–protein interaction between IRAK1 and β-TrCP was restored in CpG-treated GRko macrophages. Following 10 and 20 min of CpG and Dex cotreatment, IRAK1–β-TrCP interaction was increased by 7- and 45-fold in GRko macrophages compared with WT macrophages harboring GR (Fig. 6G).

Discussion

In the present study, we define novel mechanisms by which GC restrains TLR9-initiated inflammation via inhibition of IRAK1 ubiquitination. We provide evidence for direct physical interaction between GR and IRAK1 that interferes with protein–protein interactions between β-TrCP and IRAK1. β-TrCP–IRAK1 interaction is required for Lys linkage–specific IRAK1 ubiquitination and subsequent membrane-to-cytoplasm trafficking of TRAF6 and TAK1 facilitating NF-κB and MAPK activation (31). Additional key findings include transcription-independent rapid GC inhibition of IRAK1 ubiquitination and intracellular trafficking of TRAF6–TAK1. Furthermore, we demonstrated that GC suppression of CpG- but not LPS-induced IRAK1 ubiquitination at Lys[134] mediates anti-inflammatory effects of GC.

The genomic effects of GC occur with a delay of hours or even days after the treatment. A wealth of recent investigations have indicated that nongenomic GC actions restrict the early/acute phase of inflammatory responses (3–10). Consistent with these findings, we show that cotreatment with Dex and CpG inhibited phosphorylation of TAK1, IκBα, JNK, and p38 MAPK within 15–30 min of ligand challenge, indicating a new translation-independent mechanism of GC suppression (Fig. 1A). Cotreatment with Dex and LPS acutely suppressed p38 MAPK phosphorylation. These results are further confirmed by pharmacological inhibition of GC-dependent translation, as evidenced by persistent repression of inflammatory signals. Thus, GC targets posttranscriptional modifications in mediating acute anti-inflammatory responses.

IRAK1 ubiquitination, a posttranscriptional modification, occurs at the cell membrane (31). This modification is required for IRAK1 degradation and trafficking of TRAF6–TAK1 from the membrane

FIGURE 4. Effect of IRAK1 mutation at Lys[134] on CpG-induced K48-linked ubiquitination and degradation of IRAK1. (**A**) IRAK1^{−/−} IMM were transfected with different amounts of WT or Lys[134] mutant IRAK1 (K134R) plasmid DNA for 48 h. WCL were analyzed by immunoblotting with anti-IRAK1 and anti–β-actin Abs. (**B**) IRAK1^{−/−} IMM were transfected with WT or K134R IRAK1 DNA, followed by treatment with CpG for the indicated periods of time. WCL were immunoprecipitated with anti-IRAK1 Ab, followed by immunoblotting with anti-ubiquitin K48-linkage specific and anti–β-actin Abs. (**C**) IRAK1^{−/−} IMM were transfected with WT or K134R IRAK1 DNA, followed by exposure to CpG with or without Dex for the indicated periods of time. Dex was cotreated with the TLR ligands. WCL were analyzed by immunoblotting with anti-IRAK1 and anti–β-actin Abs. Western blots were quantified by densitometric analyses. (A and B) The abundance of IRAK1 was normalized to β-actin. IRAK1 abundance in untreated, resting IRAK1^{+/+} IMM was considered as 1 U. (C) The abundance of K48 linkage–specific IRAK1 ubiquitination was normalized to β-actin. IRAK1 ubiquitination in untreated, resting cells was considered as 1 U. The densitometry data presented are mean ± SD. Western blots are from a single experiment that are representative of three independent experiments. *p < 0.05 versus IRAK1^{−/−} IMM treated with WT IRAK1 DNA and CpG.
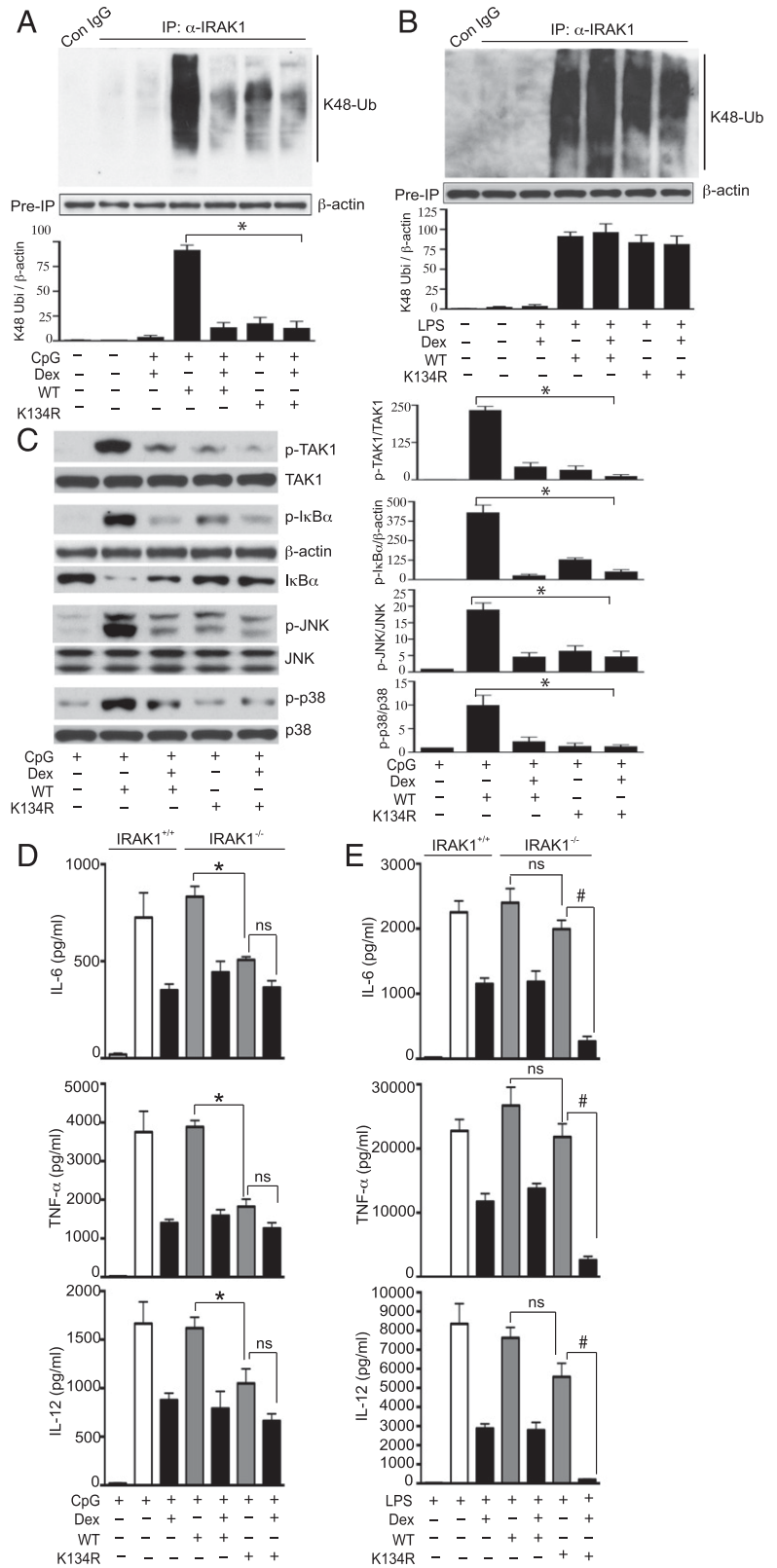
FIGURE 5. GC targets IRAK1 ubiquitination in suppressing TLR ligand–induced inflammatory actions. IRAK1$^{-/-}$ IMM were transfected with WT or K134R IRAK1 DNA, followed by exposure to (**A**) CpG and (**B**) LPS, with or without Dex for 30 min. Dex was cotreated with the TLR ligands. WCL were immunoprecipitated with anti-IRAK1 Ab, followed by immunoblotting with anti-ubiquitin K48 linkage–specific and anti–β-actin Abs. (**C**) IRAK1$^{-/-}$ IMM were transfected with WT or K134R IRAK1 DNA, followed by exposure to CpG, with or without Dex for 30 min. Dex was cotreated with the TLR ligands. WCL were analyzed by Western blot using anti–phospho-TAK1 (p-TAK1), total TAK1; anti–phospho-IκBα (p-IκBα), total IκBα; anti–phospho-JNK (p-JNK), total JNK; anti–phospho-p38 MAPK (p-p38) and total p38 MAPK (p38) Abs. All Western blots were quantified by densitometric analyses. (A and B) The abundance of K48 linkage–specific IRAK1 ubiquitination was normalized to β-actin. IRAK1 ubiquitination in untreated, resting cells was considered as 1 U. (C) Abundance of phosphorylated proteins was normalized to total protein or β-actin, as appropriate. Protein expression in untreated, resting cells was considered as 1 U. The densitometry data presented are mean ± SD. *$p < 0.05$ versus IRAK1$^{-/-}$ IMM treated with WT IRAK1 DNA and CpG. Western blots are from a single experiment and are representative of three independent experiments. (**D** and **E**) IRAK1$^{+/+}$ or IRAK1$^{-/-}$ IMM were transfected with WT or K134R IRAK1 DNA, followed by the treatment with (D) CpG or (E) LPS in the presence or absence of Dex for another 18 h. Concentrations of IL-6, TNF-α, and IL-12 in the culture media were analyzed by ELISA. Data presented as mean ± SEM from three to four independent experiments. *$p < 0.05$ versus IRAK1$^{-/-}$ IMM treated with WT IRAK1 DNA and CpG, $^{#}p < 0.05$ versus IRAK1$^{-/-}$ IMM treated with WT IRAK1 DNA and (CpG plus Dex). ns, not significant.

to the cytoplasm, where TAK1 and TRAF6 are activated. We found different Dex responsiveness for ubiquitination and stability of IRAK1 as well TRAF6–TAK1 trafficking, depending on the nature of TLR ligands. GC inhibits K48-linked IRAK1 ubiquitination and degradation/modification within 15 min of CpG but not LPS treatment. Notably, our data demonstrate acute Dex suppression of CpG-induced K48 linkage–mediated IRAK1

ubiquitination in human and mouse macrophages (in vitro), as well as in resident macrophages (in vivo) isolated from mice injected with CpG and Dex. These results suggest that Dex inhibition of K48-linked IRAK1 ubiquitination in macrophages is a conserved mechanism in mice and humans. Also, in vivo, Dex suppresses CpG- but not LPS-induced elevated plasma levels of TNF-α and IL-6, within 60 min of treatment. This rapid GC
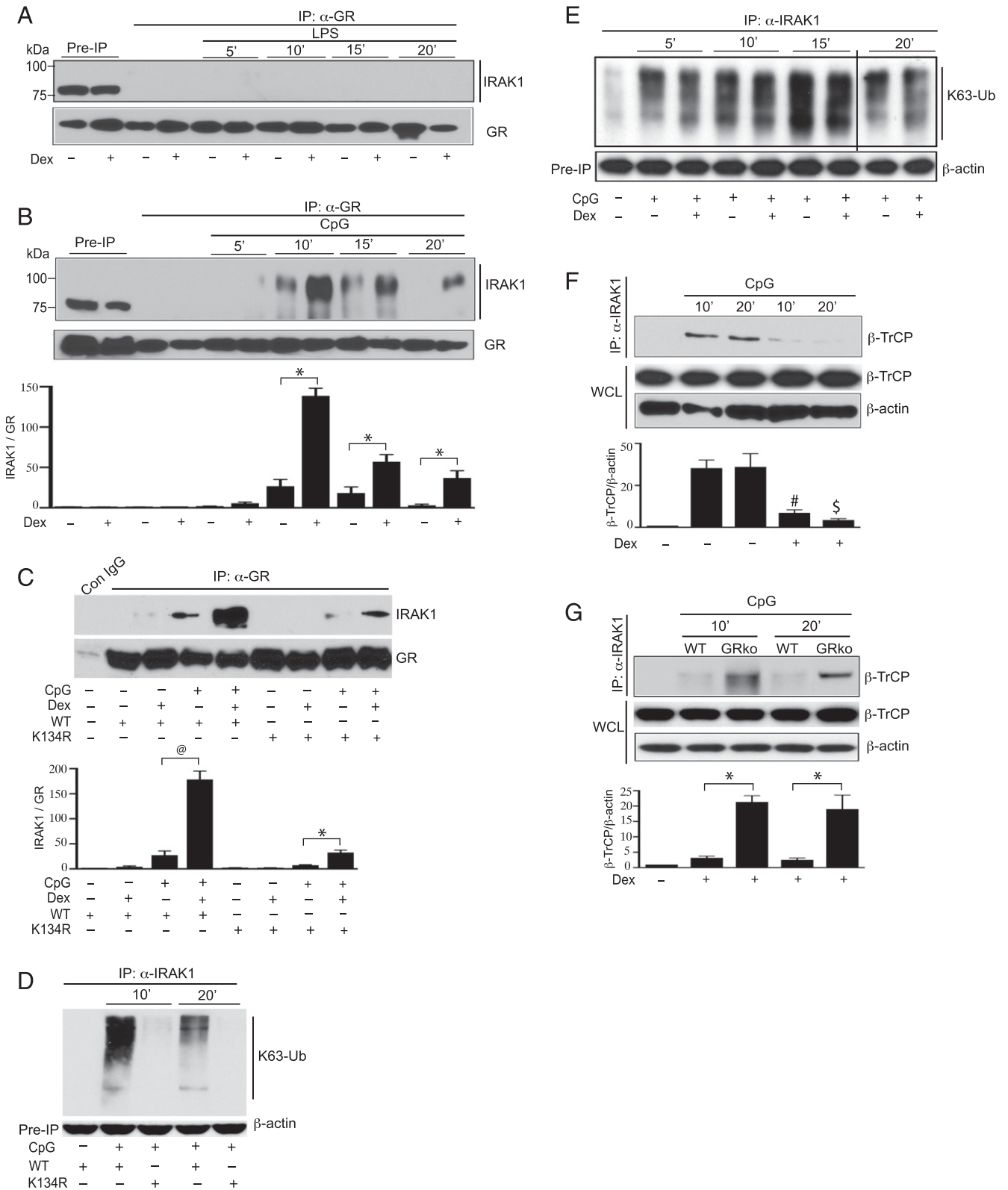
FIGURE 6. Direct physical interaction between GR and IRAK1 interferes with β-TrCP–IRAK1 interaction. Peritoneal mouse macrophages were treated with (**A**) LPS and (**B**) CpG with or without Dex for the indicated periods of time. Dex was cotreated with the TLR ligands. WCL were immunoprecipitated with anti-GR Ab, followed by immunoblotting with anti-IRAK1 and anti-GR Abs. (**C**) IRAK1$^{-/-}$ IMM were transfected with WT or K134R IRAK1 DNA, followed by exposure to CpG, with or without Dex cotreatment for 10 min. WCL were immunoprecipitated with anti-GR Ab, followed by immunoblotting with anti-IRAK1 and anti-GR Abs. (**D**) IRAK1$^{-/-}$ IMM were transfected with WT or K134R IRAK1 DNA, followed by exposure to CpG for the indicated periods of time. K63 linkage–specific IRAK1 ubiquitination in the WCL was assayed as described previously. (**E**) Mouse peritoneal macrophages were exposed to CpG, with or without Dex for the indicated periods of time. Dex was cotreated with the TLR ligands. WCL were immunoprecipitated with anti-IRAK1 Ab, followed by immunoblotting with anti-ubiquitin K63 linkage–specific Ab. The black line indicates where parts of the image are joined. (**F**) Peritoneal mouse macrophages were treated with CpG, with or without coexposure to Dex for the indicated periods of time. WCL were immunoprecipitated with anti-IRAK1 Ab, followed by immunoblotting with anti–β-TrCP and anti–β-actin Abs. (**G**) GR harboring (WT) or GR- (*Figure legend continues*)

inhibition of proinflammatory genes is distinct from the transcription-dependent inhibitory effects that result from prolonged exposure to GC and may account for subsequent inhibition from long-term GC treatment. In agreement with the inhibition of K48-linked IRAK1 ubiquitination, Dex prevented membrane-to-cytoplasm trafficking of TRAF6 and TAK1 induced by CpG but not LPS. Our data implicate that GC inhibition of CpG-induced K48-linked IRAK1 ubiquitination promotes membrane retention of TRAF6–TAK1 and prevents their subsequent trafficking to the cytoplasm.

In HeLa cells, IL-1β–induced ubiquitination at Lys^{134} is required for IRAK1 degradation/modification (43). CpG-mediated K48 linkage–specific IRAK1 ubiquitination is almost abrogated in $IRAK1^{-/-}$ IMM transfected with Lys^{134} mutant IRAK1 (K134R) DNA. Also, CpG-induced K48-linked IRAK1 ubiquitination and degradation/modification were significantly prevented in K134R IRAK1 mutant IMM. Notably, Lys^{134} on IRAK1 is required for both K48- and K63-linked IRAK1 ubiquitination (Figs. 4B, 5G); however, Dex does not inhibit CpG-induced K63 linkage–specific IRAK1 ubiquitination (Fig. 5F). Thus, via the mutation at Lys^{134} on IRAK1, we have developed a novel model to study the functional role of K48 linkage–specific IRAK1 ubiquitination. This model has been used in subsequent studies to determine the role of GC inhibition of K48-linked IRAK1 ubiquitination in mediating suppression of CpG-mediated inflammatory responses. In the absence of Dex, transfection of $IRAK1^{-/-}$ IMM with mutant IRAK1 depicts comparable inhibition of CpG-induced activation of inflammatory signal mediators (TAK1, NF-κB, JNK, and p38 MAPK) as found in Dex-treated WT IRAK1-transfected $IRAK1^{-/-}$ IMM (Fig. 5C). Moreover, the treatment of mutant IRAK1-transfected $IRAK1^{-/-}$ IMM with Dex has no additive inhibition of TAK1, NF-κB, JNK, or p38 MAPK phosphorylation (Fig. 5C). These data suggest that Dex suppression of CpG-induced K48-linked IRAK1 ubiquitination is required to inhibit the activation of inflammatory signaling cascades. The biological relevance of these results was further validated by analyzing the secretion of proinflammatory cytokines. Transfection with IRAK1 mutant demonstrated comparable inhibition of CpG-mediated IL-6, TNF-α, and IL-12 secretion as observed by Dex treatment (Fig. 5D). Consistent with the results from signaling intermediates, addition of Dex in mutant IRAK1-transfected $IRAK1^{-/-}$ IMM did not incur additional suppression of cytokine secretion. Therefore, treatment with GC or transfection with mutant IRAK1 results in a similar extent of suppression of CpG-induced inflammatory reactions. Taken together, our results suggest that inhibition of K48 linkage–specific IRAK1 ubiquitination is an important mechanism by which GC suppresses CpG-mediated inflammatory reactions, at least in cell culture.

How does GC interfere with CpG-induced K48-linked IRAK1 ubiquitination and subsequent degradation of IRAK1? Protein–protein interaction between IRAK1 and β-TrCP is required for K48 linkage–specific IRAK1 ubiquitination (31). Treatment with Dex prevents CpG-mediated IRAK1–β-TrCP interaction within 10 min of cotreatment (Fig. 6D). GC functions via GR, the cognate receptor. In the presence of Dex, interactions between IRAK1 and β-TrCP are restored in GR-deficient macrophages (Fig. 6D),

implicating inhibitory roles of GR in preventing IRAK1–β-TrCP interactions. Furthermore, in Dex and CpG cotreated cells, direct physical interaction between GR and the modified form of IRAK1 is found within 15 min of treatment. Collectively, these results suggest that direct physical interactions between GR and IRAK1 may disrupt IRAK1 interaction with β-TrCP and thereby prevent K48-linked IRAK1 ubiquitination (Supplemental Fig. 1C). Additional studies are required to map the specific GR motifs that interact with IRAK1 and substantiate the competition between GR and β-TrCP for IRAK1.

In IMM with mutant IRAK1, GR–IRAK1 interactions are inhibited after cotreatment with CpG and Dex, suggesting a requirement for IRAK1 ubiquitination in mediating these interactions. These results are unexpected because GC suppresses CpG-induced K48-linked IRAK1 ubiquitination. Recent studies implicated different linkage-specific ubiquitination of IRAK1 (31–33). In addition to K48 linkage–specific ubiquitination, IRAK1 also undergoes K63 linkage–specific ubiquitination. We hypothesize that in CpG-treated cells, IRAK1 may experiences K63-linked ubiquitination at Lys^{134}, which is unresponsive to GC treatment. In support of this notion, CpG-induced K63-linked ubiquitination of IRAK1 is strongly inhibited in K134R-transfected but not Dex-treated IMM. Our data implicate that GCs may exert a two-step mechanism to restrain CpG-induced activation of IRAK1. In the primary phase, IRAK1 ubiquitination (presumably K63 linkage specific) promotes GR–IRAK1 interaction, whereas in the late phase GCs prevent K48-linked ubiquitination of IRAK1. Further study is required to determine whether GR interacts with IRAK1 that is ubiquitinated via K63 linkage.

In sharp contrast, LPS-induced K48-linked IRAK1 ubiquitination, intracellular trafficking of TRAF6–TAK1, and activation of TAK1 are GC resistant. Also, cotreatment with Dex and LPS does not enhance physical interactions between GR and IRAK1 that we find after cotreatment with Dex and CpG. Consistently, in vivo GC fails to restrain rapid induction of TNF-α and IL-6, within 60 min of LPS treatment. Among the members of the TLR superfamily, TLR4 is unique because its engagement recruits both MyD88-MAL and/or Trif-TRAM adapter and results in a complex regulation of inflammatory reactions. It is plausible that GCs target genomic actions in restraining TLR4-initiated inflammatory responses. Furthermore, we find that GC regulation of poly(I:C)-mediated inflammatory reactions are distinct from LPS or CpG. First, unlike LPS or CpG, GC inhibition of poly(I:C)-induced TAK1, JNK, or p38 MAPK phosphorylation was reversed by CHX treatment, at least in part, indicating requirement of new translation. Second, we detected very low levels of K48-linked ubiquitination and no degradation/modification of IRAK1 in poly(I:C)-treated cells. Among TLR ligands, poly(I:C) is unique in engaging Trif-mediated signaling pathways, which trigger delayed inflammatory responses and may not require IRAK1 activation.

In this study, we demonstrated differential GC regulation of linkage-specific IRAK1 ubiquitination in macrophages depending on the nature of TLR engagement. TLR7/8 or TLR9 ligand–mediated and MyD88-dependent IRAK1 ubiquitination are GC sen-

deficient (GRko) mouse peritoneal macrophages were cotreated with CpG and Dex or left untreated. WCL were immunoprecipitated with anti-IRAK1 Ab, followed by immunoblotting with anti–β-TrCP and anti–β-actin Abs. All Western blots were quantified by densitometric analyses. Densitometry data presented are mean ± SD. (B and C) Abundance of IRAK1 was normalized to GR. GR–IRAK1 interactions in untreated, resting cells were considered as 1 U. *$p < 0.05$ versus WT macrophages treated with CpG and Dex, @$p < 0.05$ versus $IRAK1^{-/-}$ IMM treated with WT IRAK1 DNA and CpG. (F and G) Abundance of β-TrCP was normalized to β-actin. β-TrCP–IRAK1 interactions in untreated, resting cells were considered as 1 U. Western blots are from a single experiment and are representative of three independent experiments. #$p < 0.05$ versus cells treated with CpG for 10 min, $$p < 0.05$ versus cells treated with CpG for 20 min.

sitive. However, ubiquitination of IRAK1 by TLR (TLR3 or TLR4) ligands that engage TRIF is GC refractory. Degradative ubiquitination of TRAF3 in the MyD88-dependent pathway is required for the activation of MAPKs and production of proinflammatory cytokines (44). In contrast, recruitment of TRIF by TLR3 or TLR4 facilitates noncanonical auto-ubiquitination of TRAF3, which promotes IFN-dependent immune responses (44). It is plausible that the IRAK1–TRAF6 pathway is dispensable for TRIF-dependent signaling that may rely on TRAF3.

The physiological ramifications of TLR7/8 or TLR9 ligand–specific GC inhibition of IRAK1 ubiquitination are substantial. Unrestricted activation of endosomal TLRs are reported in many autoimmune diseases, including systemic lupus erythematosus (45–47). GCs are widely used in treating autoimmune diseases, including systemic lupus erythematosus (48, 49). Attenuation of IRAK1 ubiquitination would be a plausible mechanism for GC suppression of autoimmune reactions. Because IRABK1 undergoes both K63- and K48-linked ubiquitination, these studies serve as a prelude to future investigations examining specific roles of linkage-specific IRAK1 ubiquitination in inflammation. Targeting IRAK1 ubiquitination would be a novel strategy for treating many inflammatory ailments, including autoimmune disorders.

Acknowledgments

Disclosures

References

1. Buttgereit, F. 2012. A fresh look at glucocorticoids how to use an old ally more effectively. *Bull. NYU Hosp. Jt. Dis.* 70(Suppl. 1): 26–29.
2. Rhen, T., and J. A. Cidlowski. 2005. Antiinflammatory action of glucocorticoids—new mechanisms for old drugs. *N. Engl. J. Med.* 353: 1711–1723.
3. Ayroldi, E., L. Cannarile, G. Migliorati, G. Nocentini, D. V. Delfino, and C. Riccardi. 2012. Mechanisms of the anti-inflammatory effects of glucocorticoids: genomic and nongenomic interference with MAPK signaling pathways. *FASEB J.* 26: 4805–4820.
4. Stahn, C., and F. Buttgereit. 2008. Genomic and nongenomic effects of glucocorticoids. *Nat. Clin. Pract. Rheumatol.* 4: 525–533.
5. Stellato, C. 2004. Post-transcriptional and nongenomic effects of glucocorticoids. *Proc. Am. Thorac. Soc.* 1: 255–263.
6. Song, I. H., and F. Buttgereit. 2006. Non-genomic glucocorticoid effects to provide the basis for new drug developments. *Mol. Cell. Endocrinol.* 246: 142–146.
7. Kusaka, E., M. Sugiyama, N. Senoo, A. Yamamoto, and Y. Sugimoto. 2013. Genomic and non-genomic effects of glucocorticoids on allergic rhinitis model in mice. *Int. Immunopharmacol.* 16: 279–287.
8. Alangari, A. A. 2010. Genomic and non-genomic actions of glucocorticoids in asthma. *Ann. Thorac. Med.* 5: 133–139.
9. Jacobs, J. W., R. Geenen, A. W. Evers, C. H. van Jaarsveld, F. W. Kraaimaat, and J. W. Bijlsma. 2001. Short term effects of corticosteroid pulse treatment on disease activity and the wellbeing of patients with active rheumatoid arthritis. *Ann. Rheum. Dis.* 60: 61–64.
10. Lee, S. R., H. K. Kim, J. B. Youm, L. A. Dizon, I. S. Song, S. H. Jeong, D. Y. Seo, K. S. Ko, B. D. Rhee, N. Kim, and J. Han. 2012. Non-genomic effect of glucocorticoids on cardiovascular system. *Pflugers Arch.* 464: 549–559.
11. Zhou, J., Z. M. Kang, Q. M. Xie, C. Liu, S. J. Lou, Y. Z. Chen, and C. L. Jiang. 2003. Rapid nongenomic effects of glucocorticoids on allergic asthma reaction in the guinea pig. *J. Endocrinol.* 177: R1–R4.
12. Long, F., Y. X. Wang, L. Liu, J. Zhou, R. Y. Cui, and C. L. Jiang. 2005. Rapid nongenomic inhibitory effects of glucocorticoids on phagocytosis and superoxide anion production by macrophages. *Steroids* 70: 55–61.
13. Liu, L., Y. X. Wang, J. Zhou, F. Long, H. W. Sun, Y. Liu, Y. Z. Chen, and C. L. Jiang. 2005. Rapid non-genomic inhibitory effects of glucocorticoids on human neutrophil degranulation. *Inflamm. Res.* 54: 37–41.
14. Chen, K., J. Huang, W. Gong, P. Iribarren, N. M. Dunlop, and J. M. Wang. 2007. Toll-like receptors in inflammation, infection and cancer. *Int. Immunopharmacol.* 7: 1271–1285.
15. Sabroe, I., L. C. Parker, A. G. Wilson, M. K. Whyte, and S. K. Dower. 2002. Toll-like receptors: their role in allergy and non-allergic inflammatory disease. *Clin. Exp. Allergy* 32: 984–989.
16. Chinenov, Y., and I. Rogatsky. 2007. Glucocorticoids and the innate immune system: crosstalk with the Toll-like receptor signaling network. *Mol. Cell. Endocrinol.* 275: 30–42.
17. Reily, M. M., C. Pantoja, X. Hu, Y. Chinenov, and I. Rogatsky. 2006. The GRIP1:IRF3 interaction as a target for glucocorticoid receptor-mediated immunosuppression. *EMBO J.* 25: 108–117.
18. Curtale, G., T. A. Renzi, L. Drufuca, M. Rubino, and M. Locati. 2017. Glucocorticoids downregulate TLR4 signaling activity via its direct targeting by miR-511-5p. *Eur. J. Immunol.* DOI: 10.1002/eji.201747044.
19. Larangé, A., D. Antonios, M. Pallardy, and S. Kerdine-Römer. 2012. Glucocorticoids inhibit dendritic cell maturation induced by Toll-like receptor 7 and Toll-like receptor 8. *J. Leukoc. Biol.* 91: 105–117.
20. Guiducci, C., M. Gong, Z. Xu, M. Gill, D. Chaussabel, T. Meeker, J. H. Chan, T. Wright, M. Punaro, S. Bolland, et al. 2010. TLR recognition of self nucleic acids hampers glucocorticoid activity in lupus. *Nature* 465: 937–941.
21. Kong, F., G. Laryea, Z. Liu, and S. Bhattacharyya. 2015. Transforming growth factor-β-activated kinase 1 resistance limits glucocorticoid responsiveness to Toll-like receptor 4-mediated inflammation. *Immunology* 145: 136–149.
22. Bhattacharyya, S., D. E. Brown, J. A. Brewer, S. K. Vogt, and L. J. Muglia. 2007. Macrophage glucocorticoid receptors regulate Toll-like receptor 4-mediated inflammatory responses by selective inhibition of p38 MAP kinase. *Blood* 109: 4313–4319.
23. Bhattacharyya, S., C. K. Ratajczak, S. K. Vogt, C. Kelley, M. Colonna, R. D. Schreiber, and L. J. Muglia. 2010. TAK1 targeting by glucocorticoids determines JNK and IkappaB regulation in Toll-like receptor-stimulated macrophages. *Blood* 115: 1921–1931.
24. Chandra, R., S. Federici, T. Bishwas, Z. H. Németh, E. A. Deitch, J. A. Thomas, and Z. Spolarics. 2013. IRAK1-dependent signaling mediates mortality in polymicrobial sepsis. *Inflammation* 36: 1503–1512.
25. Jacob, C. O., J. Zhu, D. L. Armstrong, M. Yan, J. Han, X. J. Zhou, J. A. Thomas, A. Reiff, B. L. Myones, J. O. Ojwang, et al. 2009. Identification of IRAK1 as a risk gene with critical role in the pathogenesis of systemic lupus erythematosus. *Proc. Natl. Acad. Sci. USA* 106: 6256–6261.
26. Jain, A., S. Kaczanowska, and E. Davila. 2014. IL-1 receptor-associated kinase signaling and its role in inflammation, cancer progression, and therapy resistance. *Front. Immunol.* 5: 553.
27. Rhyasen, G. W., L. Bolanos, J. Fang, A. Jerez, M. Wunderlich, C. Rigolino, L. Mathews, M. Ferrer, N. Southall, R. Guha, et al. 2013. Targeting IRAK1 as a therapeutic approach for myelodysplastic syndrome. *Cancer Cell* 24: 90–104.
28. Burns, K., S. Janssens, B. Brissoni, N. Olivos, R. Beyaert, and J. Tschopp. 2003. Inhibition of interleukin 1 receptor/Toll-like receptor signaling through the alternatively spliced, short form of MyD88 is due to its failure to recruit IRAK-4. *J. Exp. Med.* 197: 263–268.
29. Cao, Z., W. J. Henzel, and X. Gao. 1996. IRAK: a kinase associated with the interleukin-1 receptor. *Science* 271: 1128–1131.
30. Jiang, Z., J. Ninomiya-Tsuji, Y. Qian, K. Matsumoto, and X. Li. 2002. Interleukin-1 (IL-1) receptor-associated kinase-dependent IL-1-induced signaling complexes phosphorylate TAK1 and TAB2 at the plasma membrane and activate TAK1 in the cytosol. *Mol. Cell. Biol.* 22: 7158–7167.
31. Cui, W., N. Xiao, H. Xiao, H. Zhou, M. Yu, J. Gu, and X. Li. 2012. β-TrCP-mediated IRAK1 degradation releases TAK1-TRAF6 from the membrane to the cytosol for TAK1-dependent NF-κB activation. *Mol. Cell. Biol.* 32: 3990–4000.
32. Windheim, M., M. Stafford, M. Peggie, and P. Cohen. 2008. Interleukin-1 (IL-1) induces the Lys63-linked polyubiquitination of IL-1 receptor-associated kinase 1 to facilitate NEMO binding and the activation of IkappaBalpha kinase. *Mol. Cell. Biol.* 28: 1783–1791.
33. Conze, D. B., C. J. Wu, J. A. Thomas, A. Landstrom, and J. D. Ashwell. 2008. Lys63-linked polyubiquitination of IRAK-1 is required for interleukin-1 receptor- and Toll-like receptor-mediated NF-κB activation. *Mol. Cell. Biol.* 28: 3538–3547.
34. Xiao, H., W. Qian, K. Staschke, Y. Qian, G. Cui, L. Deng, M. Ehsani, X. Wang, Y. W. Qian, Z. J. Chen, et al. 2008. Pellino 3b negatively regulates interleukin-1-induced TAK1-dependent NFκB activation. *J. Biol. Chem.* 283: 14654–14664.
35. Brewer, J. A., B. Khor, S. K. Vogt, L. M. Muglia, H. Fujiwara, K. E. Haegele, B. P. Sleckman, and L. J. Muglia. 2003. T-cell glucocorticoid receptor is required to suppress COX-2-mediated lethal immune activation. *Nat. Med.* 9: 1318–1322.
36. Clausen, B. E., C. Burkhardt, W. Reith, R. Renkawitz, and I. Förster. 1999. Conditional gene targeting in macrophages and granulocytes using LysMcre mice. *Transgenic Res.* 8: 265–277.
37. Sun, J., N. Li, K. S. Oh, B. Dutta, S. J. Vayttaden, B. Lin, T. S. Ebert, D. De Nardo, J. Davis, R. Bagirzadeh, et al. 2016. Comprehensive RNAi-based screening of human and mouse TLR pathways identifies species-specific preferences in signaling protein use. *Sci. Signal.* 9: ra3.
38. Burke, B., A. Giannoudis, K. P. Corke, D. Gill, M. Wells, L. Ziegler-Heitbrock, and C. E. Lewis. 2003. Hypoxia-induced gene expression in human macrophages: implications for ischemic tissues and hypoxia-regulated gene therapy. *Am. J. Pathol.* 163: 1233–1243.
39. Chuang, T. H., and R. J. Ulevitch. 2000. Cloning and characterization of a subfamily of human Toll-like receptors: hTLR7, hTLR8 and hTLR9. *Eur. Cytokine Netw.* 11: 372–378.
40. Du, X., A. Poltorak, Y. Wei, and B. Beutler. 2000. Three novel mammalian Toll-like receptors: gene structure, expression, and evolution. *Eur. Cytokine Netw.* 11: 362–371.
41. Kaisho, T., and S. Akira. 2003. Regulation of dendritic cell function through Toll-like receptors. *Curr. Mol. Med.* 3: 759–771.

42. Krieg, A. M., and J. Vollmer. 2007. Toll-like receptors 7, 8, and 9: linking innate immunity to autoimmunity. *Immunol. Rev.* 220: 251–269.

43. Yao, J., T. W. Kim, J. Qin, Z. Jiang, Y. Qian, H. Xiao, Y. Lu, W. Qian, M. F. Gulen, N. Sizemore, et al. 2007. Interleukin-1 (IL-1)-induced TAK1-dependent versus MEKK3-dependent NFκB activation pathways bifurcate at IL-1 receptor-associated kinase modification. *J. Biol. Chem.* 282: 6075–6089.

44. Tseng, P. H., A. Matsuzawa, W. Zhang, T. Mino, D. A. Vignali, and M. Karin. 2010. Different modes of ubiquitination of the adaptor TRAF3 selectively activate the expression of type I interferons and proinflammatory cytokines. *Nat. Immunol.* 11: 70–75.

45. Leadbetter, E. A., I. R. Rifkin, A. M. Hohlbaum, B. C. Beaudette, M. J. Shlomchik, and A. Marshak-Rothstein. 2002. Chromatin-IgG complexes activate B cells by dual engagement of IgM and Toll-like receptors. *Nature* 416: 603–607.

46. Marshak-Rothstein, A. 2006. Toll-like receptors in systemic autoimmune disease. *Nat. Rev. Immunol.* 6: 823–835.

47. Martin, D. A., and K. B. Elkon. 2005. Autoantibodies make a U-turn: the Toll hypothesis for autoantibody specificity. *J. Exp. Med.* 202: 1465–1469.

48. Chatham, W. W., and R. P. Kimberly. 2001. Treatment of lupus with corticosteroids. *Lupus* 10: 140–147.

49. Hahn, B. H. 1998. Antibodies to DNA. *N. Engl. J. Med.* 338: 1359–1368.